University of Southampton

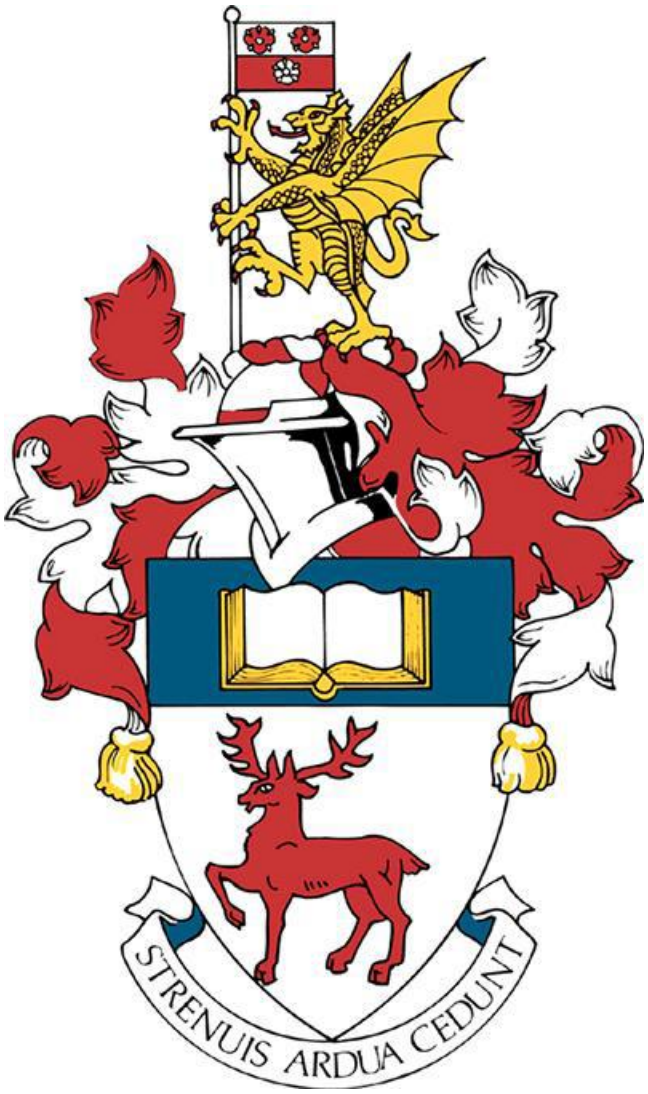

Aerodynamics of Hyperloop Transportation

by

Ritwick Varma

Student Id: 31710018

Supervisor: Dr Ralf Deiterding

Thesis for the MSc of Aerodynamics and Computation

Faculty of Engineering and the Environment

School of Aeronautics and Astronautics

24th September 2021

University of Southampton

Abstract

Aerodynamics of Hyperloop Transportation

by

Ritwick Varma

Supervisor: Dr Ralf Deiterding

Thesis for the MSc of Aerodynamics and Computation

Faculty of Engineering and the Environment

School of Aeronautics and Astronautics

The scope of the master research project hyperloop aerodynamics is studied in this report. The project mainly focuses on the flow structures, aerodynamic pressure and forces, and the shocks formed at high speeds on the hyperloop. The simulations were all performed using the software package AMROC (Adaptive Mesh Refinement for Object-oriented C++). With high-performance computing system, IRIDIS version 4.0, various scenarios were considered, and the simulations were performed. The results were then analysed using the software Visit 2.7.

Declaration of Authorship

This thesis was submitted for examination in September 2021. It does not necessarily represent the final form of the thesis as deposited in the University after examination.

I, Ritwick Varma declare that this thesis and the work presented in it are my own and has been generated by me as the result of my own original research.

I confirm that:

1. This work was done wholly or mainly while in candidature for the MSc degree at this University;

2. Where any part of this thesis has previously been submitted for a degree or any other qualification at this University or any other institution, this has been clearly stated;

3. Where I have consulted the published work of others, this is always clearly attributed;

4. Where I have quoted from the work of others, the source is always given. With the exception of such quotations, this thesis is entirely my own work;

5. I have acknowledged all main sources of help;

6. Where the thesis is based on work done by myself jointly with others, I have made clear exactly what was done by others and what I have contributed myself;

7. None of this work have been published before submission.

Table of Contents

Table of Tables

Table of figures

Acknowledgements

Firstly, I would like to thank my project supervisor Dr. Ralf Dieterding for supporting me in this project by arranging the meetings every week and guiding and motivating me to complete the project on time.

Furthermore, I would also like to thank all the post doctorates, especially Dr. Pushpender Sharma

for dedicating his time and for supporting me in learning the AMROC software.
I would also like to thank all my MSc peers for motivating me constantly and encouraging me to work hard the entire year.
Lastly, I would like to thank my parents who have been a constant supporter throughout my MSc and for this opportunity to come to UK and for helping me to fulfil one of the biggest goals of my life.

Definitions and Abbreviations

AMROC: Adaptive Mesh Refinement for Object-oriented C++

HTT: Hyperloop Transportation Technologies

ET3: Evacuated Tube Transport Technologies

Pa: Pascal

A: Area of cross section

V: Volume

P_t: Total Pressure

P_t: Total Density

T_t: Total Temperature

P: Pressure

P: Density

T: Temperature

M: Mach Number

M_{ext}: Mach number on the surface of the pod

n: Total number of panels

m: mass flow rate

m_{max}: Maximum mass flow rate

A_{bypass}: Area of cross section between the surface of the pod and the wall of the tube

A_{pod}: Area of the pod

A_{po}: Area of the pod

A_{tu} Area of the tube

BR : Blockage ratio

CAD: Computer aided design

L: Length of the pod

2D: Two Dimensional

3D: Three Dimensional

Chapter 1 Introduction

For many years the entire world has dreamt of having a reliable high-speed mode of transportation. Buses, trains, and aircraft have been successful in achieving this dream. However, the aspiration of achieving a faster transportation network has not stopped in humans. Through extensive research on making high-speed trains, the goal has not been achieved yet. This has led to an invention of a new mode of transport that is the Hyperloop. The concept of hyperloop dates to 1799 when the British Engineer George Medhurst filed a patent for inventing a system where compressed air can be used for the propulsion of goods through iron pipes. In 1909 Goddard wrote a paper called "the Limit of Rapid Transit", where he stated that it would take only 12 minutes to reach New York from Boston. He explained in his paper that fast transport could be achieved by using the concept of levitating pods and vacuum tubes. Though a physical model was not made, this paper serves as a fundamental building block for the concept of Hyperloop even today. In 2012 Elon Musk came up with the concept of the Hyperloop, which has led to a new revolutionary idea for a new mode of transportation [1].

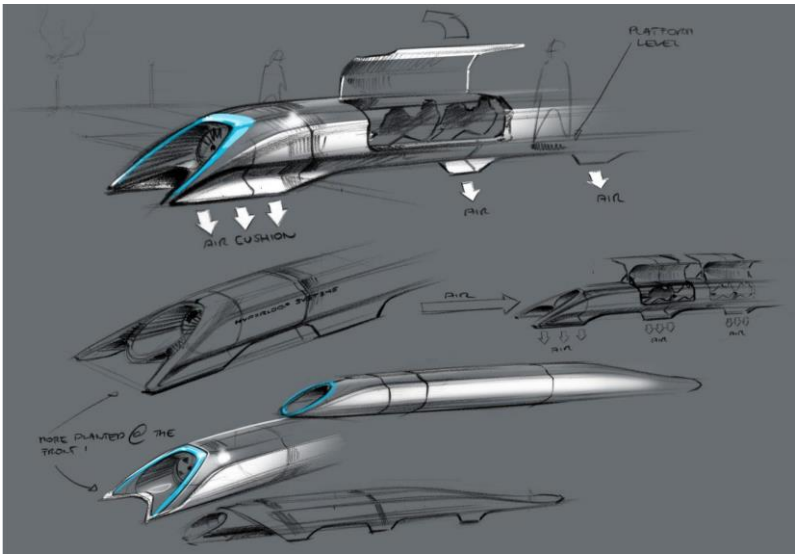

Figure 1: Sketch of Hyperloop Alpha referred from [1]

The emissions and noise pollution from automobiles have led to a significant impact on the environment and has deteriorated the health of people [2]. This has led governments of various countries worldwide to opt for electric vehicles by the year 2030. Electric vehicles do not emit any gases and are noise-free. Though it looks like a solution to the present problem, a recent estimate predicts that at least 12 million tons of lithium batteries will retire by the end of 2030 [3]. This means that there will be much waste to be dumped, creating another environmental issue.

It has also been estimated that by 2050, 47% of the transport market share will be occupied by high-speed modes of transportation [4]. The concept of Hyperloop adheres to all these requirements and is a promising mode of transport in the future.

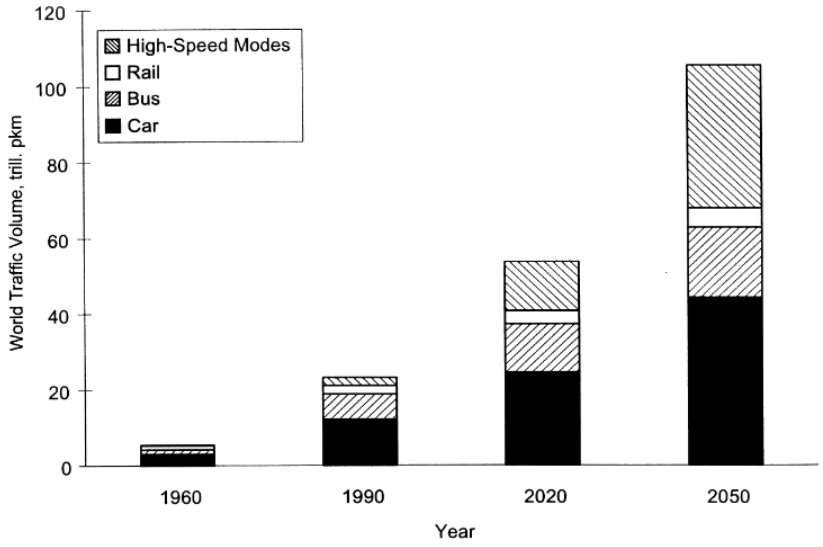

Figure 2: Estimate of future mode of mobility around the world referred from [4]

Hyperloop consists of a pod and a vacuum-tube. The pod is levitated magnetically and moves through the tube. The aerodynamic characteristics play a major role in the performance of the pod. Unlike aircrafts the pod is constricted inside the tube thus making it an internal aerodynamics problem. This has led to new challenges to overcome to achieve the performance of the pod.

Since the pod is made to move in high speeds there are two main factors that can affect its drag. They are the shock waves when the pod achieves transonic and supersonic speeds and the second one is the choking of the flow when the pod achieves critical mach number [5]. It is very important to understand the flow characteristics of the pod.

Another important factor to be considered while analysing an aerodynamic problem such as the Hyperloop is the Kantrowitz limit. Violating this limit can lead to a drastic increase in drag which will in turn lead to the loss in performance of the pod.

This project mainly deals with the understanding of the aerodynamic characteristics like the flow structure, aerodynamic forces and the shocks that will be formed at high speeds.

1.1 The Vactrain sector

The vactrain also called as the vacuum train is a design concept where the trains travel through a tube which is kept at low pressure. There have been various designs that have been considered one of which include the concept of Hyperloop.
Apart from Hyperloop there are three other major alternative players in the vactrain sectors. They are:
1. Hyperloop Technologies
2. Hyperloop Transportation Technologies (HTT)
3. Evacuated Tube Transport Technologies (ET3)
These three technologies have paved the way for the recent Hyperloop concept.

1.1.1 Hyperloop Technologies

Hyperloop Technologies was founded by Brogan Bambrogan, a former SpaceX engineer and Rob Lloyd, a former Cisco president. The company has not revealed many details of their prototype however, some of the press releases and the website reveals a few basic details of the vehicle.

Figure 3: Cargo pod designed by Hyperloop Technologies *referred from [7]*

The company currently has four test rigs. The ‘Blade Runner’ is used for the testing of axial blades of the compressor. A scaled model has been tested. A levitation rig has been created which is used to test the magnetic levitation system (Linedoll,2015). For the design validation of the tube, a big tube test rig is created for testing. The tube lab is a mobile laboratory which is used for acquiring data, modelling, and monitoring the tests. A test track has also been constructed in the Nevada desert to test the system.

1.1.2 Hyperloop Transportation Technologies

Hyperloop Transportation Technologies, HTT has been founded by Dirk Ahlborn. The funds for this project were collected through a crowdfunding by collaborating with a crowdfunding website called the Jump Starter. The company is building a test track with a distance of 8 km (Gizmag,2015). It has 200 volunteers as of 2015 working for the company and have been given shares in return.

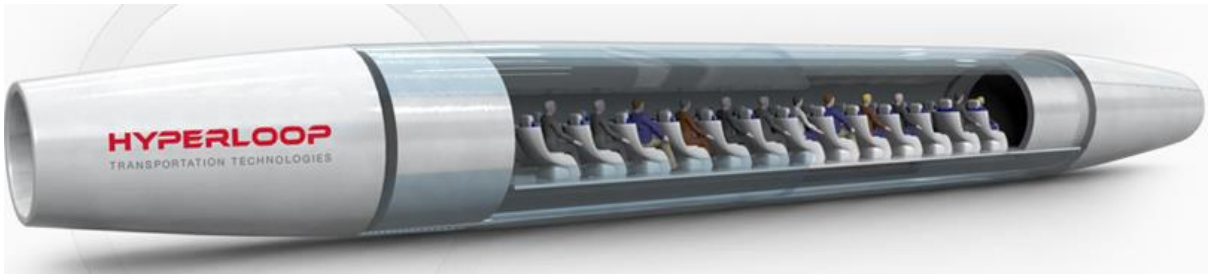

Figure 4: The *Hyperloop Pod designed by Hyperloop Transportation Technologies referred from [18]*

The Hyperloop concept of HTT is an inspiration of the Musk's concept of Hyperloop. It has a compressor at the front of the pod. A nozzle is fitted at the rear end of the pod. The tube is maintained at a pressure of 100 Pa. Though there is not much information about the project, the technical report (Ahlborn, 2014) describes the progress of the project and also provides the information about the preliminary aerodynamic study the company has performed. These aerodynamic details were missing from the original Musk's Paper.

The report also proposes to use the air bearing system for the levitation of the pod and states that this method is the most cost effective. The goal of the company is to create a Hyperloop system which can connect all the major cities in USA.

1.1.3 Evacuated Tube Transport Technologies (ET3)

Evacuated Tube Transport Technologies, ET3 has been designed and patented by Oster in 1999. The project has a tube with a diameter of 1.5 m operating at a pressure of 0.1 Pa (Vacuum pressure). The pod can accommodate 6 persons at once. It uses a linear motor for acceleration and uses a magnetic levitating system. The company uses a business model in which they sell license to operators to use this technology.

Figure 5: *Evacuated Tube Transport referred from [19]*

Compared to the original Hyperloop system, ET3 has a very small blockage ratio, and the pod has no compressor system. The system first came in 1980's and from then onwards there has been a lot of academic research on many aspects of the system. The paper written by Zhang has been a major player in the ET3 concept in the recent times.

Chapter 2 Literature Review

2.1 Governing flow

The pod travels at a very high subsonic Mach number in a tube which is of low pressure. This means that the pod travels in an environment which is low in density and low in Reynolds number. The Reynolds number is of the order 10^5, this means that there will be a transition of flow from laminar to turbulent and a transition point exist on the surface of the pod [6]. Furthermore, as the pod is travelling at high speeds which can result in many shock waves which has to be analysed carefully.

2.2 Transonic channel flow

The flow between the pod and the tunnel/tube can be considered as a flow through a small channel with the channel walls being the surface of the pod and the wall of the tube. This consideration can be taken as a supersonic nozzle which is also called as the convergent-divergent nozzle. This section is very minimum. The distribution of velocity around the pod can be considered as a result of the contraction of the area between the inlet and the void between the wall of the tube and the surface of the pod. This relationship between the velocity and the area follows the principle of conservation of mass. This relationship also gives an idea if the flow is decelerating or accelerating in the given passage. The conclusion with this relationship is that when the area of cross section decreases, it leads to the increase in the velocity of the air and eventually there will be a decrease in static pressure in a case of a subsonic flow.

The stagnation conditions are considered to be constant, and the flow is assumed as an isentropic flow. So, to get the local conditions like the temperature, density and pressure, the basic isentropic relations can be referenced. These equations are as follows:

$$\frac{\partial A}{A} = -\frac{\partial V}{V}(1 - M^2) \tag{1}$$

$$\frac{p_t}{p} = \left(1 + \frac{\gamma-1}{2}M^2\right)^{\frac{\gamma}{\gamma-1}} \tag{2}$$

$$\frac{T_t}{T} = 1 + \frac{\gamma-1}{2}M^2 \tag{3}$$

$$\frac{\rho_t}{\rho} = \left[1 + \frac{\gamma-1}{2}M^2\right]^{\frac{1}{\gamma-1}} \tag{4}$$

The relationship between the throat area and the local area can be derived from the continuity equation. Using this equation, the local Mach number can be approximated.

$$\frac{A}{A^*} = \frac{1}{M}\left[\frac{1+\frac{\gamma-1}{2}M^2}{\frac{\gamma+1}{2}}\right]^{\frac{\gamma+1}{2(\gamma-1)}} \tag{5}$$

Using all the equations above an equation can be established between the pressure coefficient, local Mach number and the freestream Mach number as shown below:

$$M^2 = \frac{2}{\gamma-1}\left[\frac{1+\frac{\gamma-1}{2}M_\infty^2}{\left(1+\frac{1}{2}\gamma M_\infty^2 C_p\right)^{\frac{\gamma-1}{\gamma}}} - 1\right] \tag{6}$$

2.3 Panel Method

Just like the channel approach, the panel method is another technique which can be used to approximate the aerodynamic properties of the pod in the Hyperloop system. The contour points are created on the surface of the pod and straight lines are drawn between the points thus dividing the surface of the pod. These divided surfaces are called as the panels.

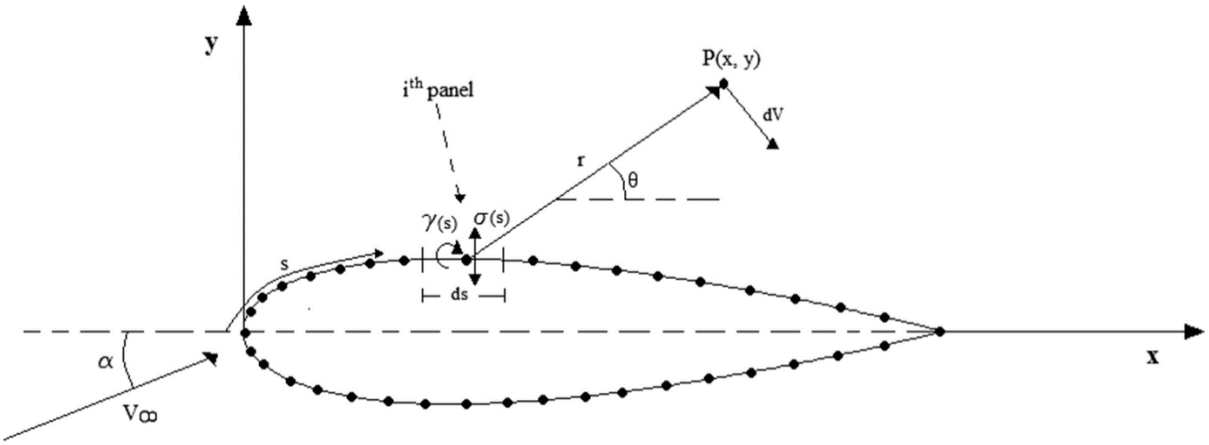

Figure 6: Source and vortex distribution over the surface of the Airfoil surface referred from [16]

Using the tangency boundary condition, the method uses a set of algebraic equations which are solved simultaneously. The following steps are used to approximate the aerodynamic properties:

1. The number of singularities is first chosen along with its type. There is an unknown strength in each singularity. So, this means that if there are n number of singularities then their n number of unknown strengths and n number of equations are required.
2. The aerodynamic surface of the pod is not discretised into n panels. These panels are of various sizes, and one must try to keep the panels to almost of the same size as that will eventually reduce the computational time. The regions on the aerodynamic surface of the pod where changes can be expected are to be identified and the panels should be concentrated in these particular regions. The

front and rear end of the pod has large curvature changes, so more panels have to be concentrated in these regions.

3. By solving the differential equations, a solution must be generated wherever the boundary condition is applied for the give case. The main aim of the panel method is to fulfil the surface tangency boundary condition. So, the boundary condition has to satisfy the n number of points on the aerodynamic surface of the pod. These n number of points are also called as the control points, and they are placed in the same way to that of the placement of singularities.

4. The fixed stream at fixed control points and the influence of all the singularities should be summed. It is important that the total local velocity is tangent to the surface at the particular control points and the normal velocity at each control point is zero. For this, the position of the control point should be kept relative to positions of the singularities and the geometrical slope of the surface. A decision should also be made as to how the singularities have to be distributed. The panel methods at higher orders provide a better accuracy when compared to the combined singularities on flat panels. But this would also mean that more computational time and cost is required.

5. For a realistic solution the Kutta condition is then implemented. The principle of Kutta conditions holds good for all steady flows. This condition ensures that the flow is smooth at the trailing edge of the pod. This means that the vorticity remains zero at the trailing edge. This condition helps in reducing one control point. This condition ca be used on a Hyperloop pod as a pod with a sharp tail is possible.

6. the system of equations generated in steps 4 and 5 can be solved. An n x n matrix is required to solve the n unknown singularity strengths. When a greater number of panels are used in this method, the final solution obtained will be more accurate. This also means that the method represents the continuous vorticity along the continuous surface more accurately.

The solution obtained from this method will be the potential flow predictions which will help in the approximation of lift. However, inclusion of the viscous component will lead to the approximation of drag on the pod. This is done by introducing a boundary layer.

2.4 Kantrowitz limit

Kantrowitz limit is an important parameter to be considered while designing the pod. This limiting condition applies to all the transportation systems which are confined to a fixed space [7]. Apart from the pod of the Hyperloop, Kantrowitz limit must be considered while designing high speed

trains which will pass through tunnels as well. The drag on the pod can increase by three times if the Kantrowitz limit is neglected [6].

Kantrowitz limit describes the amount of air that can pass through the gap between the pod and the inner walls of the tube. The tube diameter must be decided based on the limit. This can be done by the choke flow equation.

$$\mathrm{m} = \frac{Ap_t}{\sqrt{T_t}}\sqrt{\frac{\gamma}{R}}\mathrm{M}\left(1+\frac{\gamma-1}{2}M^2\right)^{\left(-\frac{\gamma+1}{2(\gamma-1)}\right)} \tag{7}$$

Where, A is the area of cross section, p_t is the total pressure, T_t is the total temperature, γ is the specific heat ratio, R is the gas constant and M is the Mach number.

The maximum flow rate happens when the Mach number is equal to 1. The equation when the flow is chocked is gives as:

$$\mathrm{m_{max}} = \mathrm{A}[\mathrm{P_o}\rho_o\gamma\left(1+\frac{\gamma-1}{2}\right)^{\left(-\frac{\gamma+1}{\gamma-1}\right)})]^{0.5} \tag{8}$$

When there is a contraction in area inside the tube, the velocity of the air increases to maintain the mass flow rate. This is governed by the equation of continuity. However, the mass flow rate can increase up to a maximum value given equation (8), beyond which flow chokes, meaning the mass flow rate can't increase even by decreasing back pressure any further for the given stagnation conditions. It can be maintained up to an extent after which the choking condition occurs. Choking happens when the flow becomes supersonic, and the velocity reaches to the speed of sound. Choking is a condition where mass flow cannot be increased more and is analogous to the venturi effect. As the air cannot through the gap between the pod and the inner wall of the tube, it will amass in front of the pod which will lead to increase in the drag of the pod. This phenomenon occurs at the throat of the reducing section [8].

There were two approaches that were considered to break the Kantrowitz limit.

- The first approach was to increase the diameter of the tube. This will eventually increase the air bypass area thus preventing the choke condition. However, this approach was not considered as increasing the diameter would mean increase in logistical cost and such a large tube will be impractical.

- The second approach was found out during the Swiss metro project in 1993. This concept includes a turbine that can be installed into the hyperloop. So, the turbine will help in drawing out the air from the front to the rear eventually avoiding choke at the cost of the power required to run the fan. This approach proved to be more practical cost efficient. This idea was also proposed in the SpaceX 2013 hyperloop project where a compressor

was placed in front of the pod. So, when the pod moves in high subsonic speeds, the fan actively draws the air from front of the pod and draws it to the rear. This eventually helped the pod to travel at a high speed of 700 mph at a relatively small tube.

The Kantrowitz limit gives the maximum bypass ratio which can be permitted before the flow changes to a supersonic flow. The bypass ratio is given by the equation (Ratnayake, 2010):

$$\frac{A_{bypass}}{A_{tube}} = \left[\frac{\gamma-1}{\gamma+1}\right]^{0.5} \left[\frac{2\gamma}{\gamma+1}\right]^{\left[\frac{1}{\gamma-1}\right]} \left[1 + \frac{2}{\gamma-1}\frac{1}{M^2}\right]^{0.5} \left[1 - \frac{\gamma-1}{2\gamma}\frac{1}{M^2}\right]^{\frac{1}{\gamma-1}} \quad (9)$$

In the above equation γ stands for specific heat capacity and M stands for Mach number. In the case of a pod inside the tube, the size of the pod should be relatively equal size of the tube. Though in such a scenario Kantrowitz limit will be exceeded, this can be overcome by reducing the pressure inside the tube to 100 Pa as proposed by Musk (2013).

2.5 Aerodynamic disturbances

In a non-lifting body like hyperloop the shockwaves must be avoided as they lead to a total pressure loss which will in turn lead to a new form of drag called the wave drag [8].
Shockwaves can also cause a separation of the boundary layer which will significantly increase the pressure drag. A wake is created between the streamlines and the body. These wakes will also lead to increase in drag of the hyperloop. Due to the rise in drag, there will be a discrepancy in the pressure distribution across the pod [9].

2.6 Hyperloop Alpha (Musk, 2013)

In this paper the pod is in the shape of a capsule is designed and is confined into a vacuum tube and is simulated to find out its aerodynamic characteristics at high speeds. The paper describes the idea of a pod that can transport 28 passengers at a very low pressure of 100 Pa. The pod is constricted inside a tube which is made of steel.

The geometry of the pod is described in the later sections and also gives an approximate aerodynamic drag that the pod can face which is 320N. It also describes about the power needed for the movement of the pod and gives a detailed explanation of the chosen 100 Pa pressure.

The paper then addresses the aerodynamic challenges. It describes about the shock waves which has to be controlled when the pod is moving close to sonic speed.

Musk's paper gives the basic details of the Hyperloop but however lacks many critical details which has led to assumption of many parameters with reference to other authors analysis.

2.7 Open-Source Conceptual Sizing Models for the Hyperloop Passenger Pod [15]

The paper discusses the thermodynamics and the aerodynamic interactions between the tube and the pod of the Hyperloop. It proposes a method of changing the blockage ratio in order to keep the pod away from the Kantrowitz limit.

The author uses a cylindrical model to increase the structural strength and decrease the aerodynamic drag. The author establishes a relation between the Mach number of the pod and the bypass air along the gap between the pod and the tube.

The conclusion made in this paper is that the Mach number has to be less than 0.65 to ensure that there is a considerable compressor efficiency at the entrance of the compressor. A diffuser is added which will help in reducing the velocity of the air. The final conclusion made in this paper is that the diameter of the tube has to be more than double than the one proposed originally so that the pod can achieve a Mach number of 0.8.

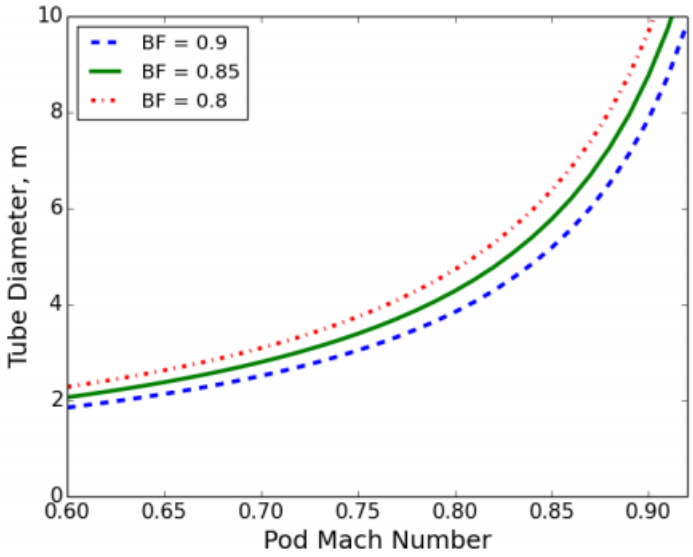

Figure 7 *Relationship of pod speed and tube diameter, for 3 blockage factors referred from [9]*

The author shows the relationship between the pod and the tube is an important factor to be considered for the design of a Hyperloop system. The idea of the Hyperloop system as proposed in this paper is more feasible compared to the original concept. This paper reveals many intricacies of Hyperloop which are missing in the initial papers.

2.8 Numerical Simulation and Analysis of Aerodynamic Drag on a Subsonic Train in Evacuated Tube Transportation [18]

The author uses a setup and uses the ETT concept for validation. The paper uses a simple pod which has a frontal area of 7.03 m^2 and the rear of the pod is kept flat. The drag force is found out for velocities in between 50 and 300 m/s at tube pressures between 1 Pa and 10000 Pa.

The study uses a 2D steady incompressible flow with the domain being 2L in the front of the pod and 2L at the rear of the pod from the pod. L is the length of the pod.
The conclusion of the paper is that the diameter of the tube should be between 2 metres and 4 metres and recommends the pressure of the air to be in between 1 Pa and 1000 Pa. This is also like the values as proposed in the original concept as proposed by Musk.
The paper provides a detailed solver setting in fluent and the geometry and gives a detailed explanation for the use of k-Ɛ turbulence model for recreating and validating for a range of meshes and to suit the problems associated with Hyperloop.

2.9 Aerodynamic Simulation of Evacuated Tube Maglev Trains with Different Streamlined Designs [14]

Different shapes have been designed by the author for the head and tail of the pod with different pressures and blockage ratio. The study concludes that the shape of the head has no much effect on the aerodynamic performance of the pod.
At 1000 Pa the blunt shape design at the tail provides a very low aerodynamic drag and blockage ratios. The semi-circular tail increases the performance of the pod even when the blockage ratio is increased by 0.25. The author uses a 2D steady incompressible flow at a speed of 300m/s and a pressure of 1000 Pa inside the tube. K-Ɛ turbulence model has been used in this analysis. The domain has been extended to 1L in the front of the pod and 2L behind the pod where L is the length of the pod

Chapter 3 Methodology

3.1 AMROC

3.1.1 Equations

AMROC solves a system of inviscid Euler equations. These equations are as follows:

$$\frac{\partial \rho}{\partial t} + \frac{\partial}{\partial x_m}(\rho u_m) = 0, \tag{10}$$

$$\frac{\partial}{\partial t}(\rho u_k) + \frac{\partial}{\partial x_m}(\rho uu + \delta_{km}\, p) = 0 \text{ , k=1,….,d} \tag{11}$$

$$\frac{\partial}{\partial t}(\rho E) + \frac{\partial}{\partial x_m}\left(u_m(\rho E + p)\right) = 0 \tag{12}$$

p stands for pressure and is in Pa, ρ stands for density and is in kg/m^3, E stands for the total specific energy and u_m is the m^{th} velocity vector component.

Another point to be noted is that in the above system of equations, pressure and density and total specific energy are always greater than 0.

The Kronecker delta δ_{km} will be 0 when k is not equal to m and will be 1 when k and m are equal.

An extra equation that is the equation of state is required to close the above equation. The equation of state is given as:

$$p = (\gamma - 1)\left(\rho E - \frac{1}{2}\rho u^2\right) \tag{13}$$

3.1.2 Mesh

The AMROC framework provides a general object-oriented approach in C++ for the block structured adaptive mesh refinement algorithm as provided in [4]. The algorithm is designed to obtain a solution for the hyperbolic partial differential equations which are of the form:

$$u_t + f(u)_x + g(u)_y + h(u)_z = s(u) \tag{14}$$

There are a variety of scales present in these kinds of problems. So, mesh refinement is very much required. The discontinuities have to found out and the smooth surfaces should be made finer. AMROC uses an adaptive cartesian and Euler mesh with fixed boundaries. The algorithm creates the coarse mesh which is then made finer. In figure 8 it can be seen how the

AMROC software refines the mesh at the region where the body is present and as well as in the compression waves region.

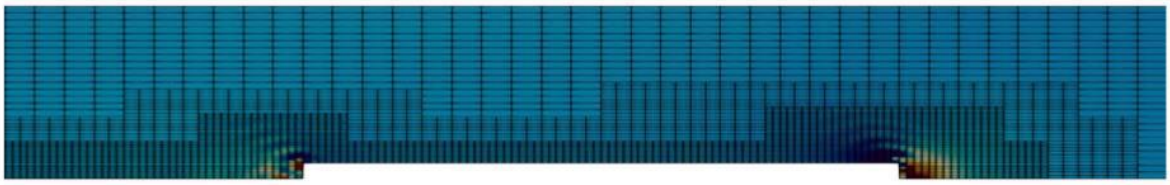

Figure 8: Aerodynamics of a high-speed train during tunnel entry and train passage referred from [22]

In cartesian mesh type the grid is built of rectangles in general (not necessarily) in case of a 2D geometry and cuboids in the case of a 3D geometry. Each cell is numbered by an integer.

3.2 Design considerations

3.2.1 Flow regime

The design of the pod used in this project was inspired by the Hyperloop-one pod. Though the pod is present inside the vacuumed tube, yet there is still some amount of air that remains inside the tube. So, it is therefore important to carefully design the pod while considering the aerodynamic parameters of the pod.

Though the pressure inside the pod is very low, the fluid that will pass through the pod is still within the continuum limit. The flow regime can be considered as unconventional as the pod moves in high speeds. The boundary of the continuum flow can be described by the dimensionless parameter called the Knudsen number, K_n. This dimensionless parameter is the ratio between the mean free path λ and the representative physical length scale of the flow [10]. The Reynolds number for this flow will be in the order of 10^5. So, when the pod moves in the tube the flow across the pod will transit from laminar to turbulent.

3.2.2 Geometry

The pod has an aeroshell design at the top which enables the air to pass through easily. The bottom part of the pod has the levitating chassis which has the propulsion system. The magnets used for levitating the pod are also embedded in this chassis. This design is like that of open wheel race cars like the formula 1.

The pod has been designed using CAD design software Solidworks. SolidWorks is a Computer Aided Design software that is published by Dassault Systemes. It is primarily intended for Windows based operating systems.

Although the geometry created is a 3D model, but an axisymmetric model of the pod is the preferred form for simulation and further studies. Although this conversion from 3D model to axisymmetric is not perfect yet it is sufficient for the analysis being done in this project.

The pod is placed in the centre of the tube is simple model an axisymmetric model has been used. This however is not the case in the real world. The pod is levitated slightly above the ground. Similarly for this analysis the tube has been taken as a circular one but, it has a concrete base [10].
The dimensions of the pod are listed in Table 1. The geometry of the pod can be seen in figures 9 and 10. The mesh of the pod can be seen in figure 11.

Table 1 Dimensions of the pod

Length of the pod (in metres)	Breadth of the pod (in metres)	Height of the pod (in metres)
8.7	2.7	2.4

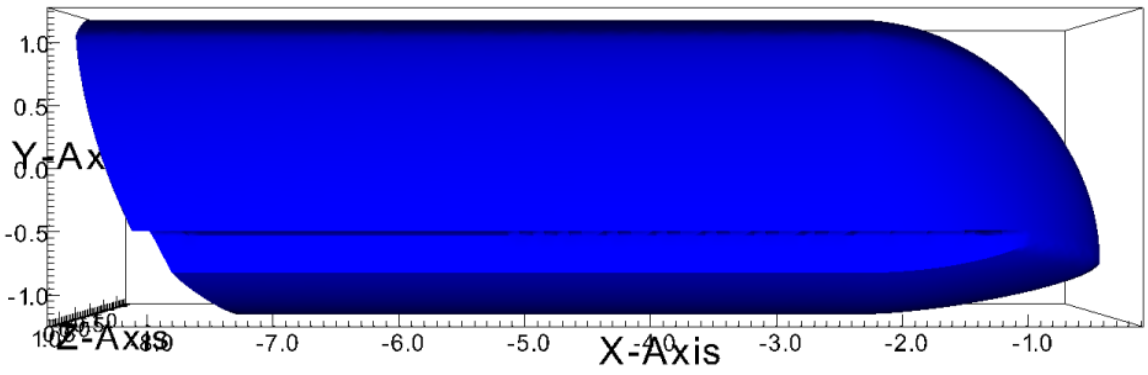

Figure 9 Side view of the designed pod

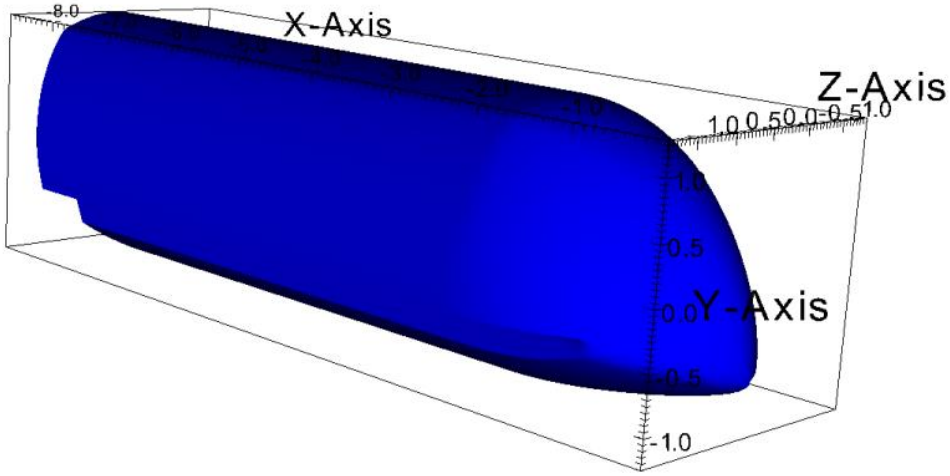

Figure 10 Isometric view of the designed pod

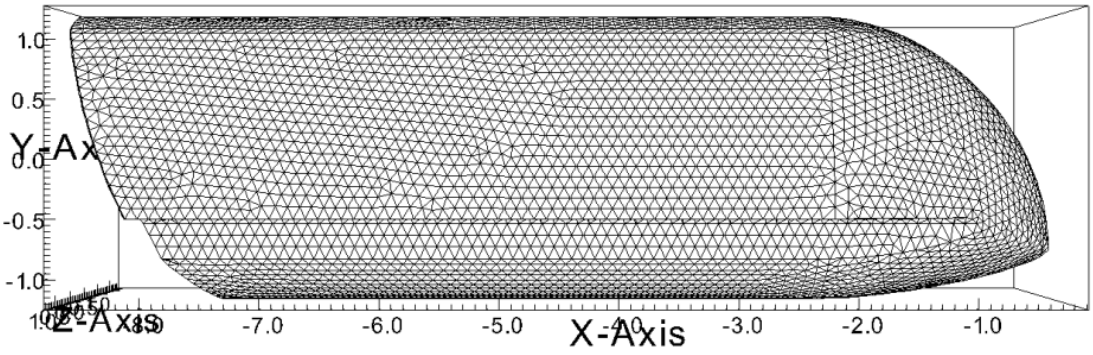

Figure 11 Side view of the pod after meshing

3.2.3 Aerodynamic design considerations

3.2.3.1 Kantrowitz limit considerations

The two ways to overcome Kantrowitz limit has been stated in section 2.2. However, both these ways have their own pros and cons. The two ways however mean that the cross-section area must be limited which will eventually increase the cost for constructing them. Adding compressors to the pod to suck the air out is very expensive and requires high maintenance. Kantrowitz limit plays a major role in the performance of the pod. It is important to consider that the created blockage ratio between the pod and the tube does not affect the performance of the pod. An analysis was done where various blockage ratios were considered and the Mach number at the flow around the pod is noted down (M_{ext}). When M_{ext} becomes 1 this is

when the flow chokes. To determine the highest speed a specific pod can move, the analysis as stated in this section is one of the main parameters to be considered.

3.2.3.2 Boundary layer separation

Since the pod is travelling in an environment with very low Reynolds number it is very easy for the boundary layer to get separated. These separations can mean an increase in the pressure drag. The skin friction drag in this case is very low, but the high pressure drag will mean that there will be large wakes behind the pod. These laminar boundary separations must be prevented. In the case of Hyperloop one this has been done by designing the nose of the pod in a way that the transition of the flow from laminar to turbulent happens right at the nose of the pod. This however led to the formation of more pressure at the front of the pod. This however has been reduced by reducing the pressure inside the tube.

3.2.3.3 Influence of the velocity

Velocity plays a major role in the performance of a pod. Since the pod is confined inside a tunnel, the pressure that develops in front of the pod will all depend upon the velocity of the pod. The waves generated and the pressure differences formed on the pod will all depend upon the velocity at which the pod is travelling. Eventually choking also takes place only at a particular velocity (or Mach number).
For this reason, an analysis has been performed where the pressure difference around the pod is analysed visually for a varying mach number. The Mach number or the velocities at which the pod was simulated ranges from Mach number 0.3 to Mach number 0.9. The Mach numbers selected for this analysis are listed below in table 1.

Table 2: Analysis of the pod performance at different Mach numbers

Analysis Number	Mach Number	Velocity (in m/s)
Analysis Number 1	0.3	102.9
Analysis Number 2	0.4	137.2
Analysis Number 3	0.5	171.5
Analysis Number 4	0.6	205.8
Analysis Number 5	0.7	240.1
Analysis Number 6	0.8	274.4

Analysis Number 7	0.9	308.7

3.2.3.4 Critical speed analysis

Ultimately, one of the most important factors to avoid exceeding of the Kantrowitz limit is to know the critical speed scenario triggering the compression waves to become a shock wave. Therefore, the main aim of these experiments was to use a range of velocities and study the changes in pressure.

To get the accurate velocity (or Mach Number) of the pod at which the flow chokes a further analysis are added as shown in table 2.

Table 3: Analysis of velocity at different Mach number to find out the critical Mach number

Analysis Number	Mach Number	Velocity (in m/s)
Analysis Number 1	0.51	175.04
Analysis Number 2	0.52	178.47
Analysis Number 3	0.53	181.90
Analysis Number 4	0.54	185.34
Analysis Number 5	0.55	188.77
Analysis Number 6	0.56	192.20

3.2.3.5 Blockage ratio analysis

Even though the pressure can be controlled in order to allow the pod to move at a high velocity the velocity can never be increased more than a certain value. The maximum velocity that the pod attains before the choke condition occurs is inversely proportional to the blockage ratio. So, the Hyperloop with a less blockage ratio will allow the pod to move in a high speed. The blockage ratio can only be increased up to a certain point or decreased up to a certain point. This is because very high blockage ratio or very less blockage ratio would not be suited in terms of monetary point of view [15].

Based on the analysis performed by Y. Zhang [12], the author proposed that the ideal blockage ratio will be in between 0.25 and 0.7.

The blockage ratio is defined as:

$$BR(\%) = \frac{A_{po}}{A_{tu}}.100 \quad (14)$$

Where A_{po} is the area of cross section of the pod and A_{tu} is the area of cross section of the tube. To understand the influence of blockage ratio on the pod three scenarios were considered in this analysis. The three blockage ratios considered are 0.25, 0.40 and 0.70. The blockage ratio is achieved by changing the radius of the tube and keeping the size of the pod constant.

Table 4: Analysis of different blockage ratio scenarios with information about the radius of the tube

Scenario	Blockage ratio	Tube radius(m)
1	0.25	2.40
2	0.40	1.90
3	0.70	1.43

3.2.3.6 Domain length analysis

The domain length analysis was done on the pod to ensure that there is no back pressure or any other parameters that are influenced from the inlet or outlet rather than the pod. With the help of the simulation environment provided by the AMROC analysis was done for different length of the tube as shown in table 4.

The pod is confined inside a cylindrical tube. Initial aim in the project is to avoid the influence of inlet, outlet, and other boundary conditions on the pod. An ideal condition would be placing the inlet and outlet at 40L away from the pod in both upstream and downstream directions where L is the length of the pod. But this would increase the computational cost which should also be reduced for an effective simulation. In domain length analysis performed by other authors, the inlet and outlet are placed very far away from the pod. Oh et al [11] has placed the inlet at 5.65L and the outlet at 1.76L, Zhang et al [12] placed the inlet 50h from the pod and the outlet at 27h from the pod where h is the heigh of the pod. Bao et al [13] placed the inlet and outlet at 31.25h and 69h respectively. Li et al [14] placed the train at 34h and 78h from the train.

Based on the above observations, inlet and outlet should be placed at 25L away from the pod. This must be verified in the following analysis.

Table 5: Different lengths of the tube taken to find out the exact length at which there is no back pressure from the inlet of the tube

Analysis Number	Length of the tube (metres)
1	50
2	100
3	150
4	160
5	170
6	180
7	190
8	200
9	250

The above analysis was done at a mach number 0.5 with pressure at 100 pascals.

3.2.3.7 Influence of pressure

To understand how the air gets compressed when the pod is moving in the tube, the aerodynamic reaction of the pod should be analysed for different pressure scenarios inside the tube. A pressure of 100 Pa has been recommended in the paper Hyperloop white [15]. When the pod is moving in transonic speeds, the movement of air in the gap between the pod and the tube will vary with varying pressure. Hence, the variation of pressure should be considered in understanding the aerodynamic characteristics of the pod. So, pressure analysis was done where the pods are tested at various velocities ranging from 100 pascal to 900 pascal at Mach number 0.55.

Table 6: Analysis of pod performance at different pressures inside the tube

Analysis Number	Pressure (in Pascal)
1	100
2	200
3	300
4	400
5	500
6	600
7	700
8	800

9	900

3.2.3.8 Mesh Sensitivity analysis

The aim of this analysis is to check the effect of mesh density on the results of the simulation. Various meshes were taken by varying the number of cells in the three axes. The drag obtained by these simulations were taken into account and compared with each other. The number of cells that were taken are listed in the table 6.
The number of cells were increased by increasing the divisions individually in all there three axes.

Table 7: Mesh sensitivity analysis for different number of cells

Analysis Number	Number of Cells
1	40,000
2	80,000
3	120,000
4	160,000
5	200,000

3.2.3.9 Multi Pod analysis

The concept of Virgin Hyperloop one is to use small pods which are a little larger than the size of the commercial family car. The reason this was chosen is to improve the connectivity and to provide the convenience on where the passenger wants to travel without changing pods in between the journey. So, in such scenarios as there will be many pods running simultaneously in the tube situations might arise where many pods have to travel one behind the other. So, it is important to analyse these scenarios. Two scenarios have been taken. One scenario involving two pods and the second scenario involving three pods.

Table 8: Scenarios taken for multi pod analysis

Analysis Number	Number of pods
1	2
2	3

These pods are placed at a distance of 15 metres apart from each other respectively.

Chapter 4 Results

4.1 Initial tests for solver verification

Tests were conducted initially to ensure that the solver is working as expected and gave a physically consistent meaningful result. The pod was placed at the centre of the tube. The tube had a total length of 80 metres with 40 metres at the back of the pod and 40 metres at the front of the pod.

The simulation were performed in AMROC with pressure at 100 Pascal and Mach number at 0.5 .

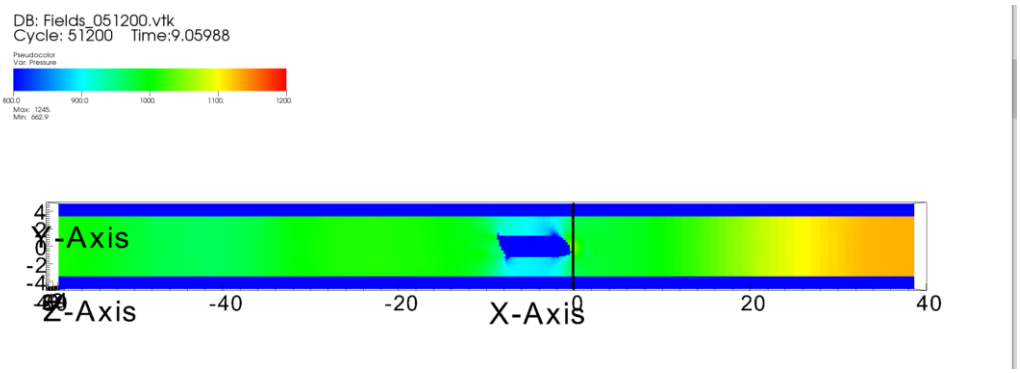

Figure 12: Testing of the solver at Mach number 0.5 with the tube pressure of 100 Pascal

Table: Mach Number 0.5

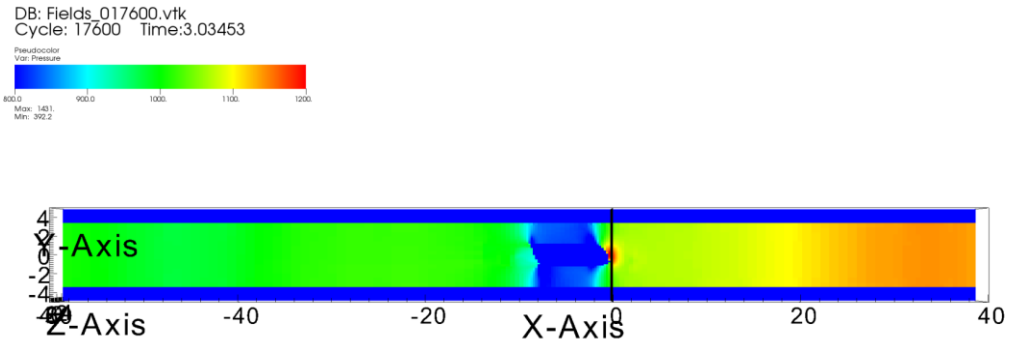

Figure 13: Testing of the solver at Mach number 0.6 with the tube pressure of 100 Pascal

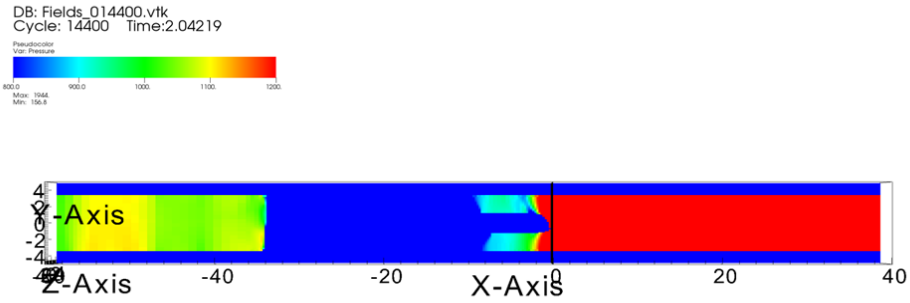

Figure 14: Testing of the solver at Mach number 0.7 with the tube pressure of 100 Pascal

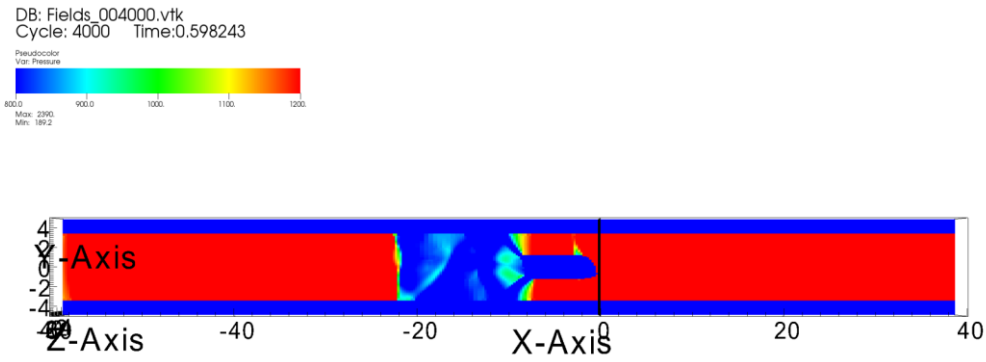

Figure 15: Testing of the solver at Mach number 0.8 with the tube pressure of 100 Pascal

According to the results from figure 9 to figure 12, it was decided to use the pressure-based steady solver for all the compressible cases. This is because this solver is considerably faster than the transient Riemann and its deviation on the drag is still lower than 1% (0.57%). Note that once the simulation is stabilized, the transient phenomena are negligible, as the standard deviation of the drag is five orders of magnitude lower than the mean value.

From the figures 9 – 12, it was observed that there has been a back flow that is starting from the inlet. The back pressure is because as the air is moving in the tube around the pod, the pressure around the pod is increasing which is eventually increasing the pressure of the air at the front of the pod. As the tube length is small at the given speed at which the pod is moving, this increase in pressure across the tube is obstructed at the inlet leading to a back pressure.

An observation that can be made in this analysis is that the pressure of air around the pod influences the pressure of air along the tube up to a certain distance.

There are two waves that are formed in a scenario like Hyperloop. They are the compression waves and the expansion waves. Compression waves are generated in the front of the pod and the expansion waves are generated at the rear of the pod when the flow becomes supersonic. These

waves are one of the reasons for the changes in pressure in the air along the pod apart from the shape of the pod and the tunnel confinement creates this flow distribution around the pod.[10]. Through this analysis one conclusion was made that it is necessary to find out the exact length of the tube that is required for further analysis so that this length is sufficient for the compression and expansion waves to pass through without forming any reflections from the inflow or outflow boundaries that can affect the results of the simulations.

4.2 Domain Length analysis

As, stated in 4.1 the domain length analysis is required to ensure that the compression waves and the expansion waves do not hit the inlet or outlet respectively causing unwanted reflections that can affect the results of the simulation.

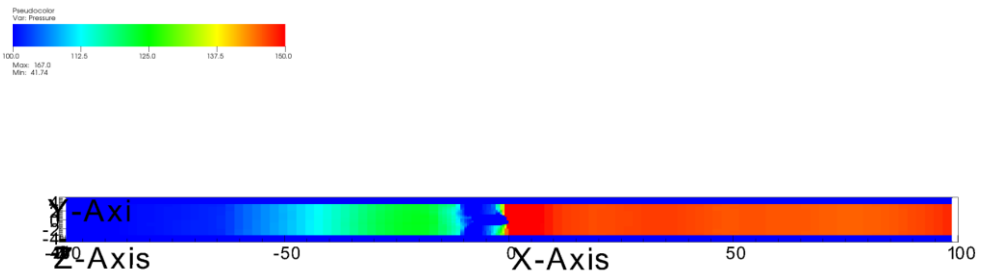

Figure 16: Domain length analysis with the length of the tube of 100 metres at the front and rear of the pod with pressure at 100 Pa.

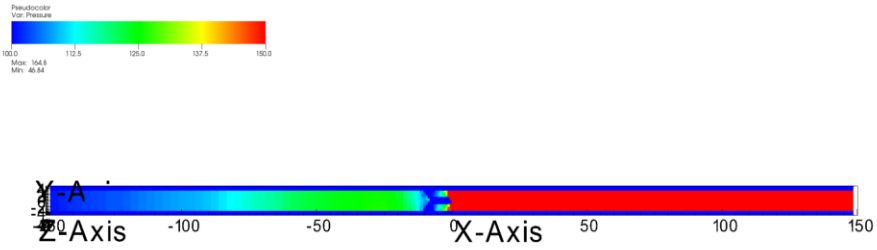

Figure 17: Domain length analysis with the length of the tube of 150 metres at the front and rear of the pod with pressure at 100 Pa.

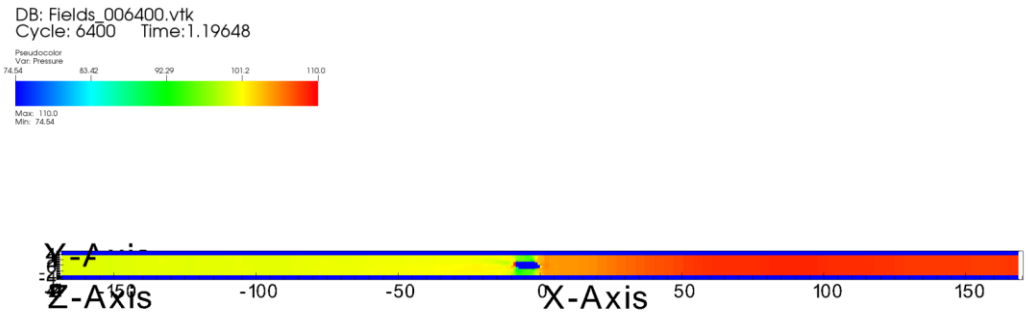

Figure 18: Domain length analysis with the length of the tube of 160 metres at the front and rear of the pod with pressure at 100 Pa.

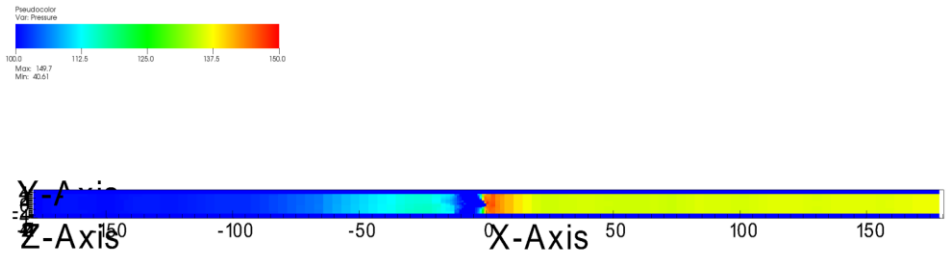

Figure 19: Domain length analysis with the length of the tube of 180 metres at the front and rear of the pod with pressure at 100 Pa.

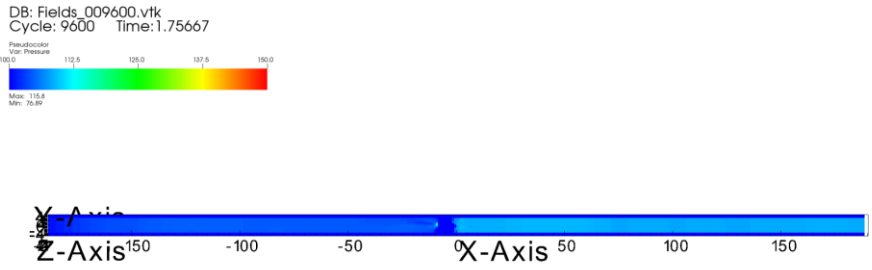

Figure 20: Domain length analysis with the length of the tube of 190 metres at the front and rear of the pod with pressure at 100 Pa.

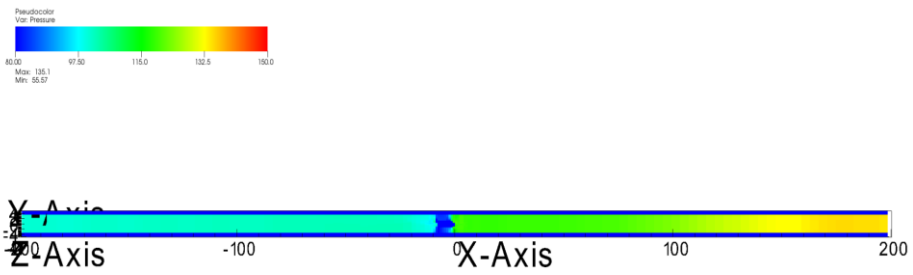

Figure 21: Domain length analysis with the length of the tube of 200 metres at the front and rear of the pod with pressure at 100 Pa.

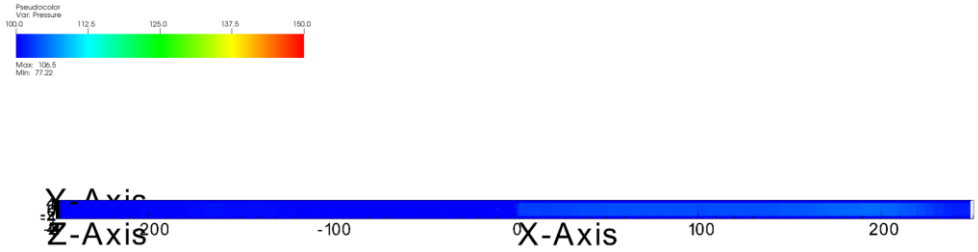

Figure 22: Domain length analysis with the length of the tube of 250 metres at the front and rear of the pod with pressure at 100 Pa.

From this analysis, it was observed that there was back pressure up to 170 metres. From domain length 180 metres, the results had no influence of any back pressure. Further analysis at domain lengths 190 metres, 200 metres and 250 metres showed that there was no back pressure influence on the results.

For further analysis, the domain length has been taken as 200 metres i.e. is the inlet is placed 200 metres in front of the pod and the outlet is placed at a distance of 200 metres from the pod. As the length of the pod is 8.7 metres, the distance considered is 22.98L which also matches to the other authors considerations as stated in 3.2.3.6.

4.3 Mesh Sensitivity analysis

Upon careful analysis of the pressure contours of all scenarios, one observation made is that with the increase in the number of cells the pressure contours are more clearly visible, and it becomes easy to get a clear picture of the pressure differences around the pod. However, the computational time increases with increase in the cells.

All the results were taken at a time stamp of 5 seconds.

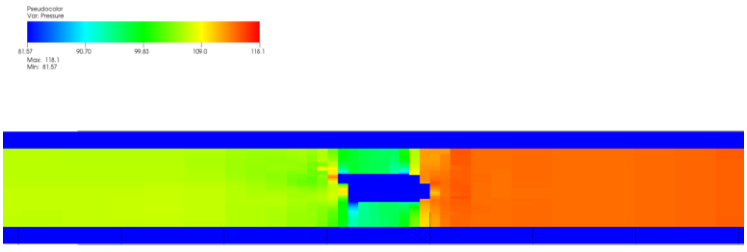

Figure 23: Pressure contour of the pod with 40,000 cells at a pressure of 100 Pa

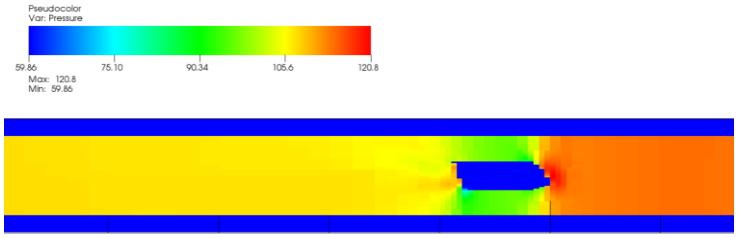

Figure 24: Pressure contour of the pod with 80,000 cells at a pressure of 100 Pa

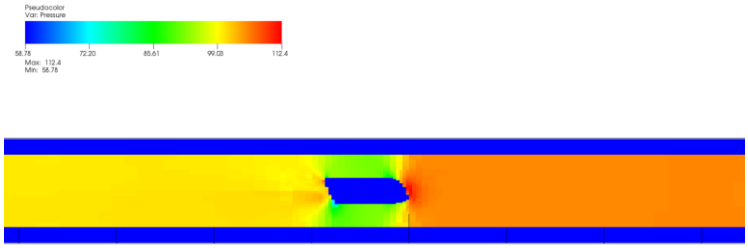

Figure 25: Pressure contour of the pod with 120,000 cells at a pressure of 100 Pa

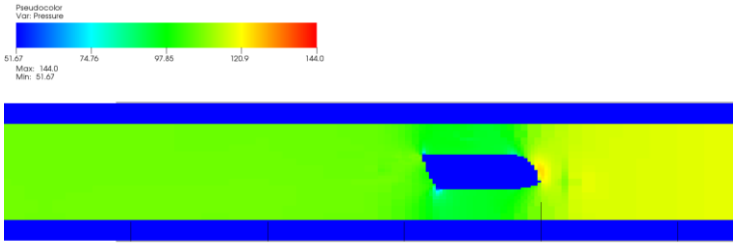

Figure 26: Pressure contour of the pod with 160,000 cells at a pressure of 100 Pa

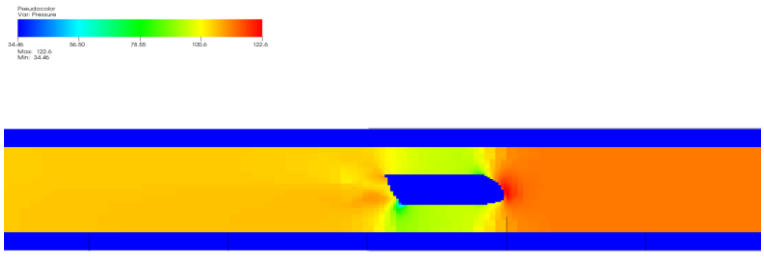

Figure 27: Pressure contour of the pod with 200,000 cells at a pressure of 100 Pa

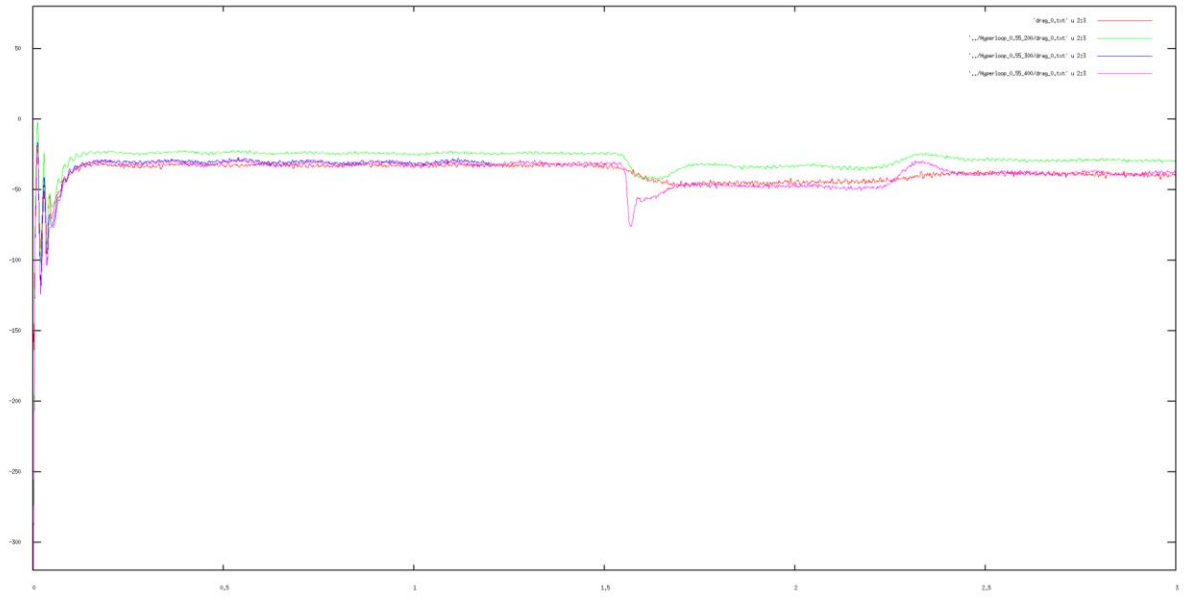

Figure 28: Plot between drag force of the pod with respect to time for the cases with different meshes

In figure 25, the green line represents the drag force of the pod in the scenario where the mesh has 40,000 cells. The red line represents the drag force of the pod in the scenario where the mesh has 80,000 cells. The purple line represents the drag force of the pod in the scenario where the mesh has 120,000 cells. The pink line represents the drag force of the pod in the scenario where the mesh has 160,000 cells.

The drag increased with the increase in number of cells. However, the drag remained same for the number of cells above 80,000. So, for the further analysis the mesh with 80,000 cells have been taken. Though the mesh with a greater number of cells will give a better result, it will also increase the computational cost. The results obtained at the number of cells 80,000 are sufficient for this study.

4.4 Blockage ratio analysis

The initial blockage ratio analysis was performed at a Mach number 0.5. The Mach number on the pod at the location where the shocks will occur has been noted down as shown in table 8.

Table 9: The external Mach number on the pod for different blockage ratio scenarios at Mach number 0.5

Scenario	Blockage Ratio	External Mach number (M_{ext})
1	0.25	0.85

2	0.40	0.72
3	0.70	0.60

The analysis was then done for Mach number 0.3 and 0.8 at a pressure of 100 Pa inside the tube.

Table 10: The external Mach number on the pod for different blockage ratio scenarios at Mach number 0.3

Scenario	Blockage Ratio	External Mach number (M_{ext})
1	0.25	0.54
2	0.40	0.43
3	0.70	0.35

Table 11: The external Mach number on the pod for different blockage ratio scenarios at Mach number 0.8

Scenario	Blockage Ratio	External Mach number (M_{ext})
1	0.25	1.1
2	0.40	0.95
3	0.70	0.79

From the table 8, table 9 and table 10 the results clearly indicate that it is important to consider a suitable blockage ratio and at the same time a suitable Mach number at which the pod will move. At Mach number 0.8 at a blockage ratio of 0.25, the flow of air between the surface of the pod and walls of the tube has exceeded Mach number 1 (critical speed). So, this is a case that should never be considered.

4.5 Influence of velocity

When the pod passes through the tube at a high speed, a high-pressure region is formed in the front of the pod nose. Meanwhile, the pod tail experiences an increase in the velocity of flow and reduces the pressure behind the pod. This phenomenon is similar to the behaviour of flow through a convergent–divergent nozzle and results in a greater pressure difference between the nose and the tail of the pod; this leads to an increase in the pressure drag.

Since the major aim in the design of the hyperloop has always been to make the pod run at a very fast speed it is very important to consider the aerodynamic performance of the pod. Based on the mentioned cases in 3.2.3.3 the following graph was obtained as shown in figure 26.

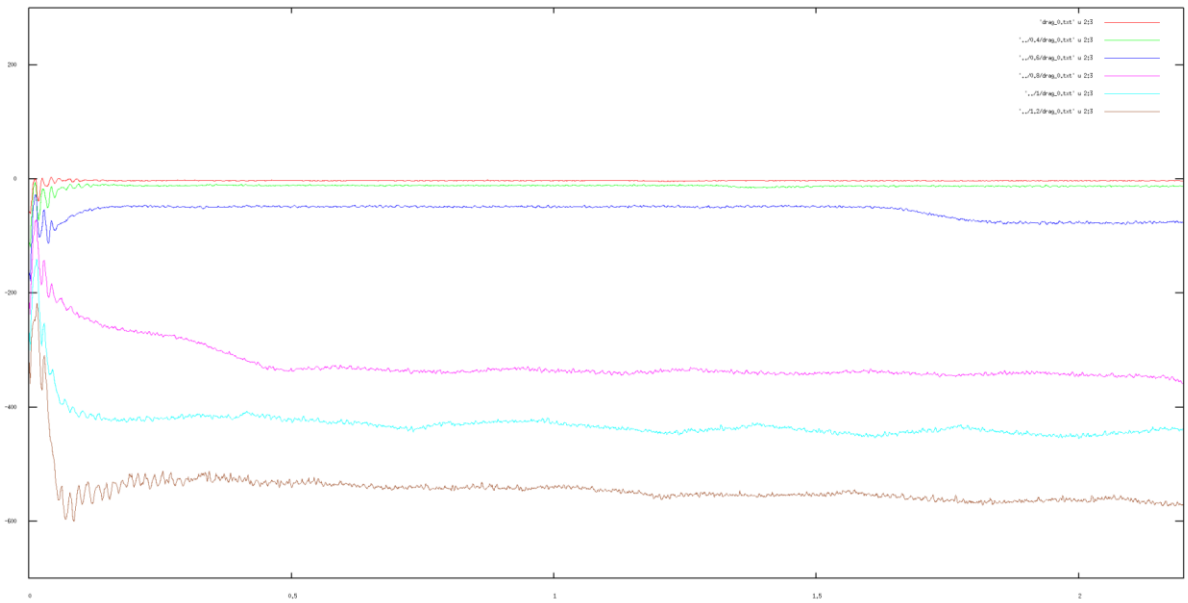

Figure 29: Plot between drag force of the pod with respect to time for the cases with different Mach numbers at a contact pressure of 100 Pa

In figure 26, the red line represents the drag force of the pod at Mach number 0.2. The green line represents the drag force of the pod at Mach number 0.4. The purple line represents the drag force of the pod at Mach number 0.6. The pink line represents the drag force of the pod at Mach number 0.8. The blue line represents the drag force of the pod at Mach number 1. The brown line represents the drag force of the pod at Mach number 1.2.

From the figure 26 it has been observed that with the increase in the velocity there is an increase in the drag. This is mainly due to the pressure build-up in front of the pod which decreases the aerodynamic performance of the pod by increasing the drag. It can also be observed that there is a drastic increase in drag from mach number 0.6. This means that the pod has reached a critical speed somewhere in between 0.5 and 0.6. In order to find out the exact critical Mach number of the pod a further analysis was done with mach numbers 0.51,0.52,0.53,0.54,0.55,0.56 and the mach number is noted down at the point on the pod where the shock wave will form. This is demonstrated in figure 29.

4.6 Critical speed analysis

In order to find out the exact critical speed of the pod a further analysis was done with mach numbers 0.51,0.52,0.53,0.54,0.55,0.56 and the mach number is noted down at the point on the pod where the shock wave will form. This is demonstrated in figure 27.
The critical Mach number condition was reached at Mach number 0.56 or 192 m/s. So, the maximum safe speed the pod can move is at Mach number 0.55 that is at 188.77 m/s at a blockage ratio of 0.25.
The pod starts behaving like a piston at Mach numbers greater than 0.56. This can be seen in figure 30 where the drag of the pod at Mach number 0.56 increases drastically. In such a scenario the pod starts behaving like a piston. The drag appearing from the pressure differential increases exponential independent of the initial pressure of the air in the tube.

Table 12: External Mach number on the pod for given scenarios with different Initial Mach numbers

Scenario	Mach Number	External Mach Number
1	0.51	0.58
2	0.52	0.65
3	0.53	0.79
4	0.54	0.86
5	0.55	0.93
6	0.56	1.04

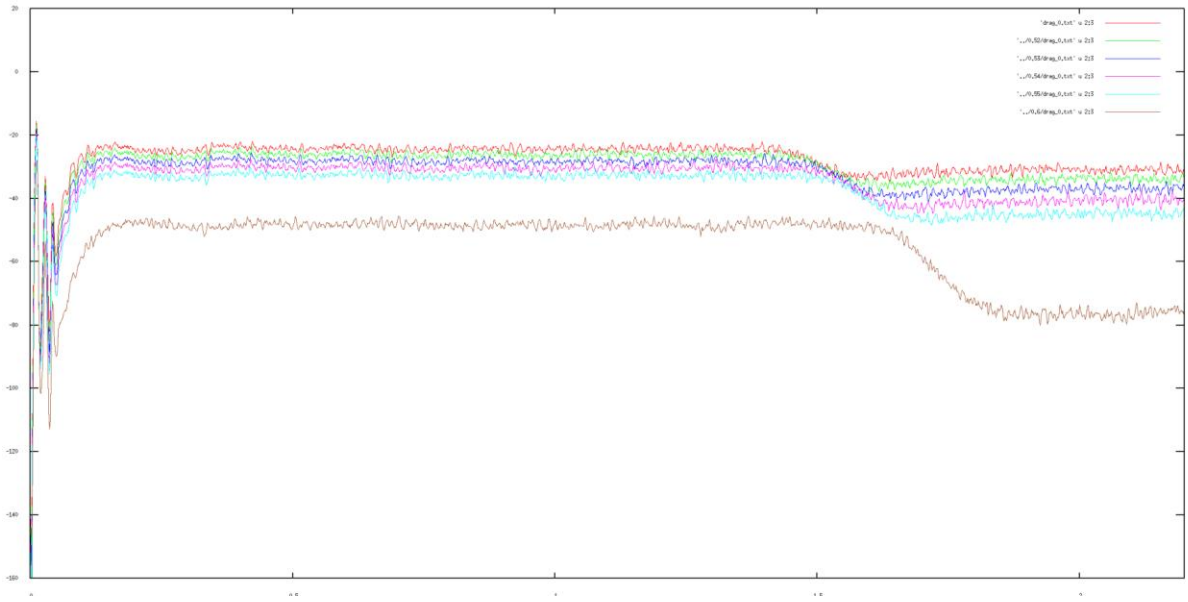

Figure 30: Plot between drag force of the pod with respect to time for the cases with different Mach numbers at a constant pressure of 100 Pa to find out the critical Mach number

In figure 27, The red line represents the drag force of the pod at Mach number 0.51. The green line represents the drag force of the pod at Mach number 0.52. The purple line represents the drag force of the pod at Mach number 0.53. The pink line represents the drag force of the pod at Mach number 0.54. The blue line represents the drag force of the pod at Mach number 0.55. The brown line represents the drag force of the pod at Mach number 0.56.

4.7 Influence of pressure

The pressure contours generated on the pod clearly shows the increase in pressure in front of the pod as the pod moves at high speeds. The graph in figure 31 clearly shows that with the increase in pressure the drag on the pod increases. This will eventually affect the aerodynamic performance of the pod. So, it is necessary to maintain the tube at a very low pressure that is at 100 bar as stated by Musk (2013). There is also a presence of a choked flow as the pressure increases and plunger effect. The presence of these parameters solely depends on the pressure inside the tube. As it is necessary to avoid these parameters the pressure inside the tube should be kept very low. But low pressure means that more energy is required by the fan to move the pod. So, a compromise must be made between the pressure of the tube and the velocity of the pod such that the choked flow doesn't happen and at the same time less energy is utilised by the fan for the movement of the pod.

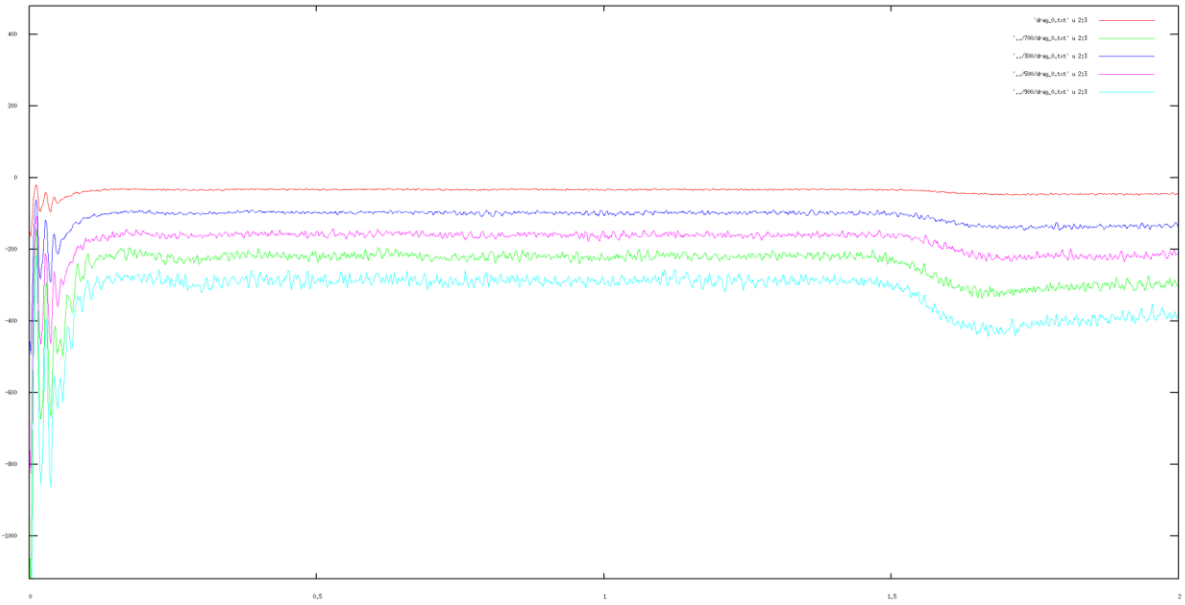

Figure 31: Plot between drag force of the pod with respect to time for the cases with different pressures at a Mach number of 0.5

In figure 28, The red line represents the drag force of the pod at Mach number 0.5 and the pressure of the tube at 100 Pa. The purple line represents the drag force of the pod at Mach number 0.5 and the pressure of the tube at 300 Pa. The pink line represents the drag force of the pod at Mach number 0.5 and the pressure of the tube at 500 Pa. The green line represents the drag force of the pod at Mach number 0.5 and the pressure of the tube at 700 Pa. The blue line represents the drag force of the pod at Mach number 0.5 and the pressure of the tube at 900 Pa.

4.8 Multi pod analysis

4.8.1 Multi pod analysis with two pods

The analysis clearly shows that the drag on the second pod is less than that of the first pod. As the air flows by the first pod, a wake is formed by the first pod which eventually reduces the pressure in front of the second pod. This leads to a decrease in the drag of the second pod. The pressure in front of the first pod and the second pod are as shown in table 13.

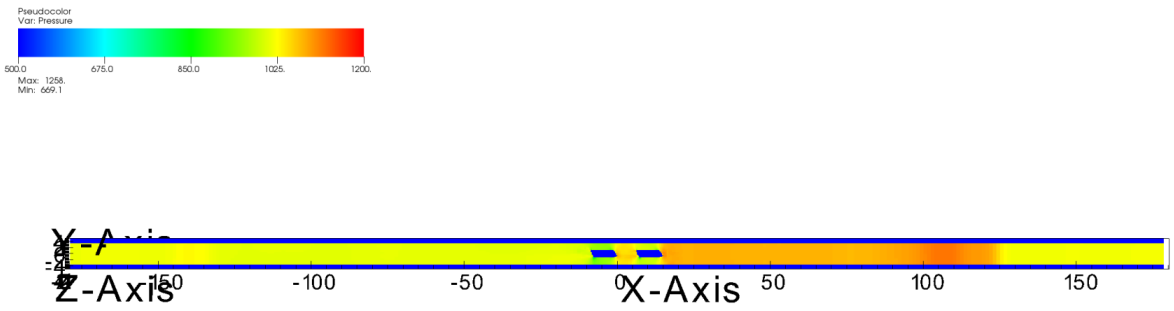

Figure 32: Pressure contour of the multi pod analysis with two pods

Table 13: External Mach number and the pressure in front of the two pods in the multi pod analysis

Pod	Pressure in front of the pod (Pa)	External Mach Number
1	161.53	0.53
2	118.70	0.27

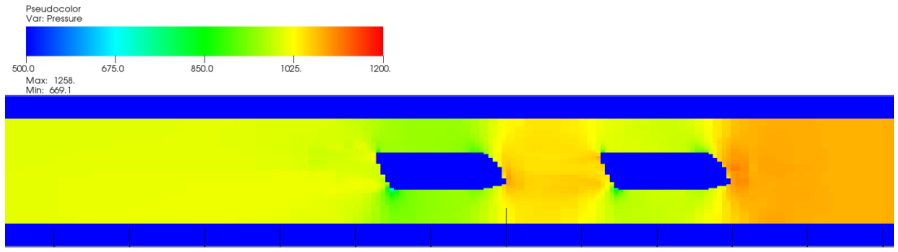

Figure 33: Pressure difference between the two pods leading to the decrease in drag of the second pod

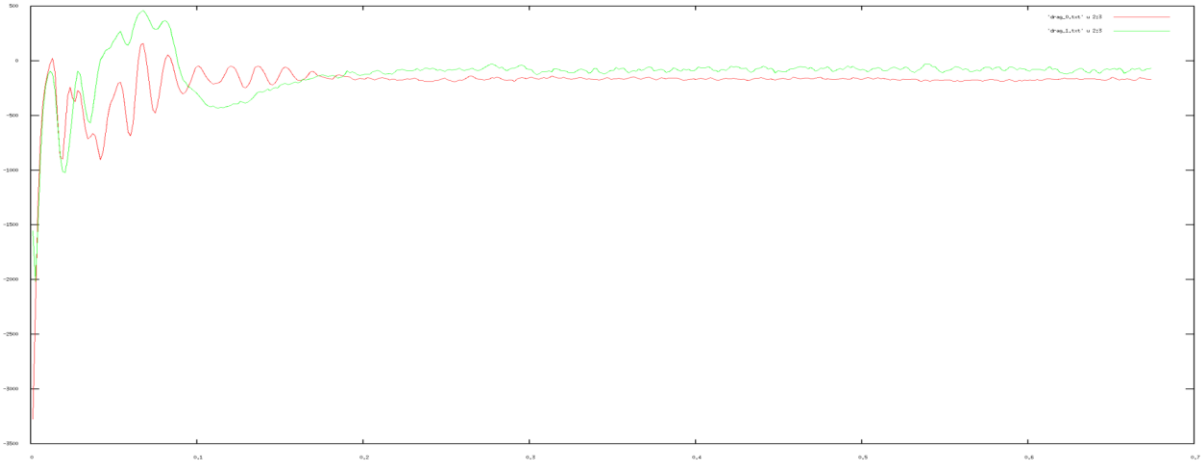

Figure 34: Plot of drag force with respect to time of the two pods

In figure 31, The green line represents the drag force of the first pod and the red line represents the drag force of the second pod.

4.8.2 Multi pod analysis with three pods

The analysis of three pods shows that the drag force on the second pod drastically reduces as it is drafting the first pod. However, the drag force on the third pod is same as the first pod. This means that the influence of the wake of the first pod can only be felt by the second pod. As the pressure difference between the front and the rear end of the second pod is very less, the drag force on the third pod is more than that of the second pod almost equal to that of the first pod.

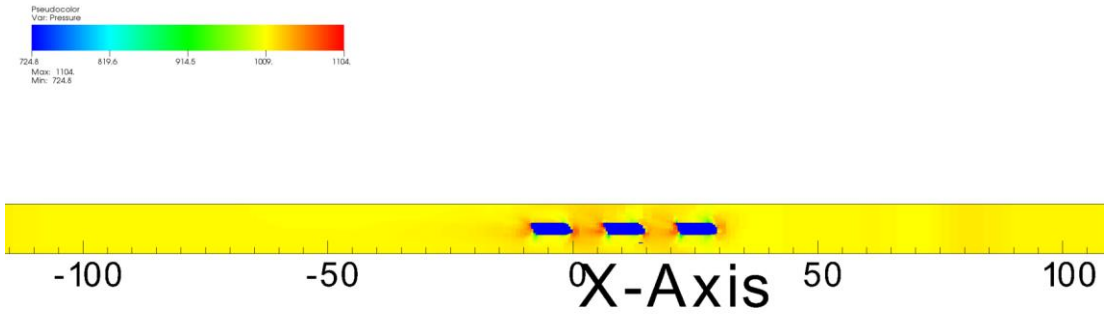

Figure 35: Pressure contour of the multi pod analysis with three pods

Table 14: External Mach number and the pressure in front of the three pods in the multi pod analysis

Pod	Pressure in front of the pod (Pa)	External Mach Number
1	163.80	0.54
2	116.53	0.29
3	152.96	0.35

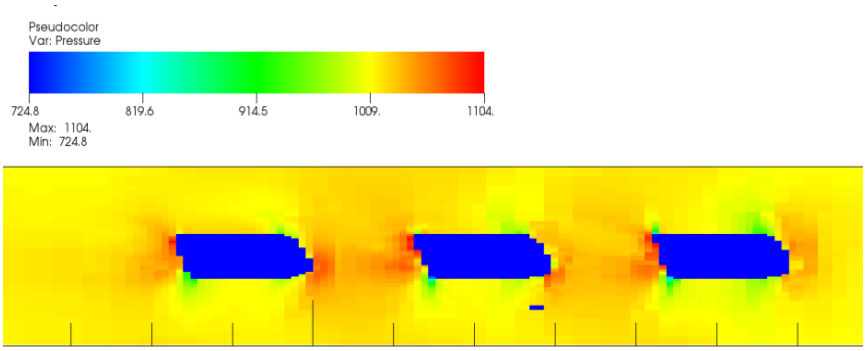

Figure 36: Pressure difference between the three pods leading to the decrease in drag of the second pod and considerable same drag force in the third pod

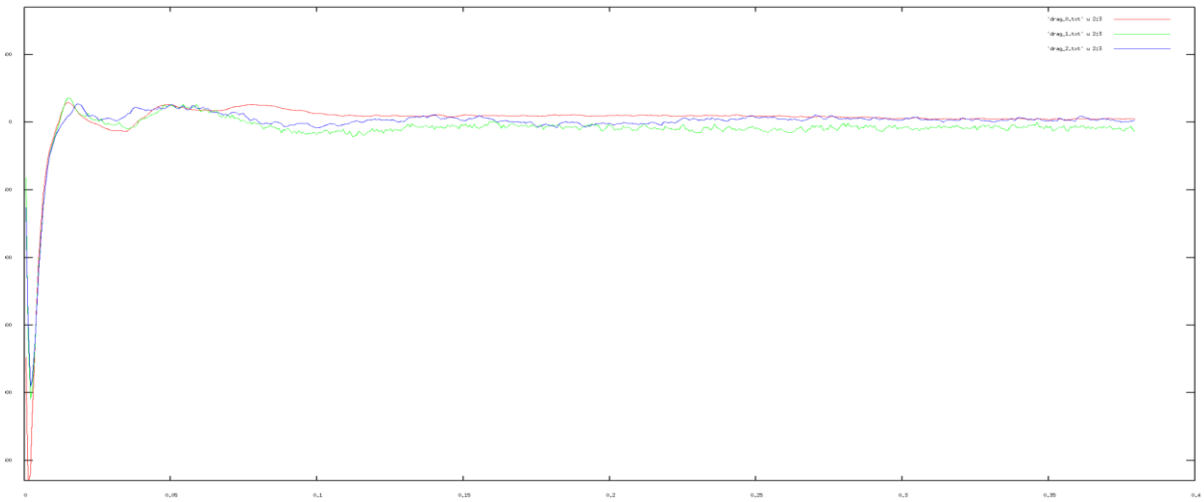

Figure 37: Plot of drag force with respect to time of the three pods

In figure 34 the red line represents drag force of the first pod, the green line represents the drag force of the second pod and the purple line represents the drag force of the third pod.

Chapter 5 Conclusions and Recommendations

5.1 Conclusions

The in house AMROC aerodynamic solver is used in performing the CFD simulations and the solver was verified. The initial CFD simulations obtained are deemed as a reliable proof for the verification of the solver for the present problem. The flow behaviour across the pod has been studied and various aerodynamic parameters are analysed. The changes in the flow of air were mainly observed in front of the pod specially at the nose of the pod.

From the analysis one conclusion is that the aerodynamic parameters that are very important for the design of a pod are the blockage ratio, velocity and the pressure inside the tube (operating pressure). The shape of the pod can drastically affect the blockage ratio. Though the shape of the pod is fixed in a simulation, a study should always be done to analyse the most suitable shape of the pod ensuring that the blockage ratio is maintained as needed and the further analysis are proceeded.

When an internal flow problem is being analysed one of the important parameters is the development of the boundary layer. Since the operating pressure is very low, the Reynolds number will be low. This leads to the reduction of the bypass area between the surface of the pod and the walls of the tube. The transition to turbulent occurs in the mid-section of the pod will lead to decrease in the throat area which results in choke of the flow.

The large pressures noticed at the front of the pod is due to exceeding of the Kantrowitz limit which is also due to the choking of the flow. The velocity of air increases in the region between the surface of the pod and the walls of the tube. In order to ensure that the Kantrowitz limit does not exceed it is important that this flow does not exceed the critical Mach number.

The velocity with which the pod travels also plays a major role. Based on the velocity analysis done as shown in figure 26 and figure 27 the pod taken in this thesis can go up to a maximum speed of Mach number 0.55. Exceeding this speed will lead to exceeding the Mach number. This is evident in Figure 27 where the drag force of the pod drastically increases at Mach number 0.56 when compared to the drag on the pod at Mach number 0.55.

The pressure analysis performed clearly shows that the pod can travel at high speeds in low operating pressures. But this would also mean that more power is needed to propel the pod. If power is not a concern, then the best operating pressure will be 100 Pa based on the analysis done in this thesis. If power is a concern, then the operating pressure has to be increased from 100 Pa to a point where the power can be afforded.

The idea of moving pods one behind the other looks possible based on the analysis done in this thesis. It has been observed that the pod behind the first pod will have a lesser drag force. However, this process of drafting is not effective for many pods. When the pods are moving one behind the other at a distance of 15 metres from each other, the second pod experiences a reduction in drag. However, the pods behind the second pod have no effect or a drastic change in drag due to the first pod. Once conclusion ca be made that this idea by Virgin Hyperloop seems to be a possible concept based on the analysis done in this thesis.

5.2 Recommendations

Since the pressure inside the tunnel is maintained by the means of a device outside the tunnel, an analysis can be done to check the aerodynamic behaviour of the pod when the device fails and the pressure starts varying.

An analysis can be made to understand the aerodynamic behaviour of the pod as it accelerates from rest.

To reduce the plunger effect, fins shaped in the form of an aerofoil can be attached to the pod. This will eventually reduce the drag force on the pod. Since the pod is operated using maglev, there might be a possibility of a negative lift considering the design of the pod. A positive lift can be generated using these aerofoils. The aerofoils will also reduce the formation of eddies and also reduces the pressure that forms in front of the pod.

Although the focus has been in simulating a maglev pod, an emphasis must be given in designing a pod with wheels. The student projects like the MIT Hyperloop project have already shown the possibility of a high-speed pod with wheels. Research must be carried out on the wheels that can sustain the frictions and heat generated in such high speeds. Pneumatic tires are very much favourable for the pod. However, there is no proper design of pneumatic tire yet that can be used on the pod.

The accuracy of the results can be improved by improving the solver. Since boundary layer plays a major role in the distribution of velocity and the distribution of other parameters in regard to flow a focus on improving the solver in terms of these aspects can increase the accuracy of the solver drastically. The current solver though provides accurate results a better solver will benefit in the optimization process.

A deep investigation must be performed in selecting an accurate position of the transition and the choking at the inlet. This can be done by improving the mesh quality. This would also increase the computational cost. Due to this limitation a considerable mesh was used.
Recommendations can be made in the multi pod analysis. Though this thesis gives a basic understanding of the changes in the flow of air around the pods a greater number of pods can be placed one behind the other and simulated. The gap between the pods has been taken as 15 metres. Another analysis can be considered where in different scenarios can be considered where the gaps between the pods can be increased and decreased as well and analysing the flow around the pods. With such analysis a conclusion can be made as to what is the minimum distance the pods have to maintain between each other.

References

1. E. Musk, Hyperloop Alpha, URL: ”http://www.spacex.com/sites/spacex/files/hyperloop_alpha-20130812.pdf”, [cited 3 May 2017]
2. McCubbin, D.R. and Delucchi, M.A., 1999. The health costs of motor-vehicle-related air pollution. *Journal of Transport Economics and Policy*, pp.253-286.
3. TheGuardian,URL:”https://www.theguardian.com/environment/2021/aug/20/electric-car-batteries-what-happens-to-them”, [cited 24 August 2021] (2021).
4. Schafer, A. and Victor, D.G., The future mobility of the world population, Transportation Research Part A: Policy and Practice 34, 171 (2000).
5. Lluesma-Rodríguez, F., González, T. and Hoyas, S., 2021. CFD Simulation of a Hyperloop Capsule Inside a Low-Pressure Environment Using an Aerodynamic Compressor as Propulsion and Drag Reduction Method. *Applied Sciences*, *11*(9), p.3934.
6. M. Opgenoord and P. Caplan, On the Aerodynamic Design of the Hyperloop Concept, American Institute of Aeronautics and Astronautics , 1 (2016).
7. Kantrowitz, A.; Donaldson, C. Preliminary investigations of supersonic diffuser, duP. Naca WR L 1945, 713, 2–11.
8. Ross, P.E., 2015. Hyperloop: no pressure. *IEEE Spectrum*, *53*(1), pp.51-54.
9. Manisankar, C. and Verma, S.B. and Raju, C., Shock-Wave Boundary-Layer Interaction Control on a Compression Corner Using Mechanical Vortex Generators, 28th International Symposium on Shock Waves , 409 (2012).
10. Wang, Y., Yang, G., Huang, C. and Wang, W., 2012. Influence of tunnel length on the pressure wave generated by high-speed trains passing each other. *Science China Technological Sciences*, *55*(1), pp.255-263.
11. Oh, J.S.; Kang, T.; Ham, S.; Lee, K.S.; Jang, Y.J.; Ryou, H.; Ryu, J. Numerical Analysis of Aerodynamic Characteristics of Hyperloop System. Energies 2019, 12, 518.
12. Zhang, Y. Numerical simulation and analysis of aerodynamic drag on a subsonic train in evacuated tube transportation. J. Mod. Transp. 2012, 20, 44–48.
13. Bao, S.; Hu, X.; Wang, J.; Ma, T.; Rao, Y.; Deng, Z. Numerical study on the influence of initial ambient temperature on the aerodynamic heating in the tube train system. Adv. Aerodyn. 2020, 2, 28.
14. Li, T.; Zhang, X.; Jiang, Y.; Zhang, W. Aerodynamic Design of a Subsonic Evacuated Tube Train System. Fluid Dyn. Mater. Process. 2019, 15, 121–130.

15. Singh, Y.K. and Mehran, K., 2019. Numerical analysis for aerodynamic behaviour of hyperloop pods.
16. Oueslati, M.M., Dahmouni, A.W. and Nasrallah, S.B., 2018. Aerodynamic Performances of Pitching Wind Turbine Airfoil Using Unsteady Panel Method. In *Exergy for A Better Environment and Improved Sustainability 1* (pp. 443-471). Springer, Cham.
17. J. Anderson, Fundamentals of Aerodynamics, 5th ed. (McGraw-Hill, 1221 Avenue of the Americas,New York, NY 10020, 2011).
18. Majchrzak, A., Griffith, T.L., Reetz, D.K. and Alexy, O., 2018. Catalyst organizations as a new organization design for innovation: The case of hyperloop transportation technologies. *Academy of Management oster*, *4*(4), pp.472-496.
19. Oster, D., Kumada, M. and Zhang, Y., 2011. Evacuated tube transport technologies (ET3) tm: a maximum value global transportation network for passengers and cargo. *Journal of Modern Transportation*, *19*(1), pp.42-50.
20. Opgenoord, M.M. and Caplan, P.C., 2018. Aerodynamic design of the hyperloop concept. *Aiaa Journal*, *56*(11), pp.4261-4270.
21. Chen, X., Zhao, L., Ma, J. and Liu, Y., 2012. Aerodynamic simulation of evacuated tube maglev trains with different streamlined designs. *Journal of Modern Transportation*, *20*(2), pp.115-120.
22. Jose Miguel Garro Fernandez , 2017. Aerodynamics of a high-speed train during tunnel entry and train passage, MSc Thesis , University of Southampton, Southampton